Development 122, 671-682 (1996)
Printed in Great Britain © The Company of Biologists Limited 1996
DEV9455

The *C. elegans* gene *vab-8* guides posteriorly directed axon outgrowth and cell migration

Bruce Wightman[1,*], Scott G. Clark[3], Anna M. Taskar[1], Wayne C. Forrester[1], Andres V. Maricq[3], Cornelia I. Bargmann[2,3] and Gian Garriga[1]

[1]Department of Molecular and Cell Biology, University of California, Berkeley, CA, 94720-3204, USA
[2]Howard Hughes Medical Institute and [3]Programs in Developmental Biology, Neuroscience, and Genetics, Department of Anatomy, University of California, San Francisco, CA 94143-0452, USA

*Author for correspondence (e-mail: wightman@mendel.berkeley.edu)

SUMMARY

The assembly of the nervous system in the nematode *C. elegans* requires the directed migrations of cells and growth cones along the anteroposterior and dorsoventral body axis. We show here that the gene *vab-8* is essential for most posteriorly directed migrations of cells and growth cones. Mutations in *vab-8* disrupt fourteen of seventeen posteriorly directed migrations, but only two of seventeen anteriorly directed and dorsoventral migrations. For two types of neurons that extend axons both anteriorly and posteriorly, *vab-8* mutations disrupt only the growth of the posteriorly directed axon. *vab-8* encodes two genetic activities that function in the guidance of different migrations. Our results suggest that most posteriorly directed cell and growth cone migrations are guided by a common mechanism involving the *vab-8* gene.

Key words: anterior-posterior axis, axon guidance, cell migration, pathfinding, *C. elegans*, *vab-8* gene

INTRODUCTION

The migrations of neurons and their growth cones shape the structure and connectivity of developing nervous systems. Notable examples include the migrations of neural crest cells to generate the peripheral nervous system of vertebrates (Le Douarin, 1980) and the radial migrations of neurons that form the layers of the mammalian cortex (O'Rourke et al., 1992; Walsh and Cepko, 1993). In addition, extensive migrations of growth cones generate the axonal patterns of connectivity required for nervous system function (Goodman and Shatz, 1993).

Growth cones and migrating cells navigate through complex environments to reach their destinations by responding to guidance cues provided by other cells and the extracellular matrix. These cues include cell-associated molecules, immobilized matrix components and diffusible molecules. In vivo and in vitro studies have defined activities that stimulate or inhibit axon outgrowth nondirectionally, and directional activities that attract or repel migrating cells and growth cones (Reichardt and Tomaselli, 1991; Keynes and Cook, 1995). A major goal of developmental neurobiology is to understand how these cues are provided and interpreted as well as how individual cells integrate information from multiple cues.

Genetic analysis of the nematode *Caenorhabditis elegans* has identified a guidance mechanism that provides directional information along the dorsoventral axis to migrating cells and growth cones. The product of the *C. elegans* gene *unc-6* acts as a directional cue for both dorsally and ventrally directed migrations (Hedgecock et al., 1990; McIntire, et al., 1992). *unc-6* encodes a secreted, laminin-related protein that has been proposed to be distributed in a gradient along the dorsoventral axis (Hedgecock et al., 1990; Ishii et al., 1992). The *unc-5* gene is specifically required for dorsally directed migrations and appears to encode an UNC-6 receptor (Leung-Hagesteijn et al., 1992; Hamelin et al., 1993).

UNC-6 is closely related to the netrins, vertebrate proteins that act in vitro as chemotropic molecules for commissural growth cones in the developing spinal cord (Tessier-Lavigne et al., 1988; Kennedy et al., 1994; Serafini et al., 1994). netrin-1 is secreted by the ventral floor plate cells, suggesting that a gradient of netrin activity might direct commissural growth cones ventrally to the floor plate. Therefore, one cue that functions in guiding circumferential migrations appears to be functionally conserved between species (Goodman, 1994).

Although components involved in directing circumferential (dorsoventral) migrations have been identified, relatively little is known about the molecules involved in directing longitudinal (anteroposterior) migrations. Longitudinal axon outgrowth and cell migration is a prominent feature of the development of the *C. elegans* nervous system. Most neuronal cell bodies in *C. elegans* are located in ganglia of the head and tail or ventrally along the length of the animal (Fig. 1; Albertson and Thomson, 1976; White et al., 1976, 1986). Many of these neurons extend axons along the main longitudinal nerve bundles, the ventral and dorsal nerve cords, while others extend longitudinal axons along several smaller lateral nerve bundles.

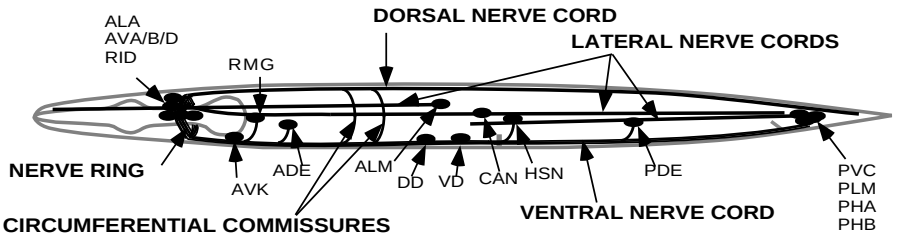

Fig. 1. A diagram (left lateral view) of the adult hermaphrodite *C. elegans* nervous system, indicating the location of neurons and axon bundles examined in this paper. The major axon bundles include the nerve ring, which encircles the pharynx, and the longitudinal ventral and dorsal nerve cords, which extend the length of the animal. Smaller axon tracts include the lateral nerve cord bundles and circumferential commissures. Arrows indicate the locations of cell bodies. There are 13 VD and 6 DD neurons in an adult hermaphrodite; one example of each cell type is shown. AVA, AVB, AVD, AVK, and PDE extend axons posteriorly along the ventral nerve cord. HSN, PDE, PHA, PHB and PVC extend axons anteriorly along the ventral nerve cord. ALA and CAN extend axons posteriorly along a lateral nerve cord. ALM, CAN and PLM extend axons anteriorly along lateral nerve cords. RID extends an axon posteriorly along the dorsal nerve cord. ADE, HSN, RMG and PDE extend axons ventrally, while DDn and VDn extend axons dorsally to form circumferential commissures.

In addition, several cell bodies migrate from the head or tail to specific positions along the length of the body.

Mutations in the *vab-8* (*v*ariable *ab*normal morphology) gene were shown previously to impair the longitudinal migrations of three cell types (Manser and Wood, 1990). Here, we describe in detail the role of *vab-8* in guiding the migrations of cells and growth cones along the anteroposterior body axis. Our results indicate that mutations in *vab-8* disrupt most posteriorly directed migrations, yet they fail to perturb most circumferential and anteriorly directed migrations. Based on *vab-8* mutant phenotypes, we propose that *vab-8* acts in the production or interpretation of a global longitudinal guidance cue.

MATERIALS AND METHODS

Strains and genetics

Standard methods of culturing and handling animals were used (Brenner, 1974). The *vab-8* alleles *e1017* and *ct33*, and the uncoordinated (Unc), withered-tail (Wit), multivulva (Muv), and protruding vulva (Pvl) phenotypes have been previously described (Manser and Wood, 1990). We also noted that many *vab-8* mutants are constipated (Con; see Thomas, 1990). The *vab-8* alleles *gm84* and *gm99* are EMS-induced mutations isolated in screens for mutants with displaced CANs (W.C.F., F. Wolf and G.G., unpublished results). *ev411* was identified in a screen for Unc mutants (J. Culotti, personal communication) and formerly defined the gene *unc-107*. Our results indicate that *ev411* is a *vab-8* allele: *ev411* causes defects in axon outgrowth like other *vab-8* mutations (Table 1), maps to the same 0.3 mu interval as *vab-8* mutations (B.W., A.M.T., and G.G., unpublished results), and fails to complement *vab-8(ct33)* for the Unc phenotype (Table 2).

Heteroallelic heterozygotes were constructed by mating *vab-8/+* males to *dpy-11(e224) vab-8(ct33)* hermaphrodites (3.7 mu separate *dpy-11* and *vab-8*). Non-Dpy F_1 progeny were scored for Vab-8 phenotypes. The presence of *gm84* or *ev411* in the putative heteroallelic F_1 progeny was confirmed by placing individual F_1 progeny onto separate Petri plates and examining the F_2 for the presence of 3/4 Vab non-Dpy and 1/4 Vab Dpy progeny. Animals hemizygous for *vab-8* and the genetic deficiency *ctDf1* were constructed by mating *ev411/+*, *gm84/+*, or *rh205/+* males to *ctDf1/nT1 unc(n754dm)* hermaphrodites. F_1 animals that did not display the dominant Unc phenotype caused by *nT1* (*n754dm*) were scored for Vab-8 phenotypes. The presence of the *vab-8* mutation was verified by placing individual F_1 progeny onto separate Petri plates and examining the F_2 progeny for the absence of wild-type animals.

Two additional *vab-8* alleles were identified by their failure to complement the *vab-8(ct33)* mutation. *lon-3(e2175)* males were mutagenized with EMS (Sulston and Hodgkin, 1988) and mated to *dpy-11(e224) vab-8(ct33) V; xol-1(y9) X* hermaphrodites. The *xol-1* mutation kills males and was included to prevent mating among the F_1 progeny. The cross progeny (non-Dpy) were screened for hermaphrodites that displayed the Vab-8 Unc or Wit phenotypes. Animals homozygous for new *vab-8* mutations were isolated by picking Lon F_2 animals. From 5320 F_1s screened, two new *vab-8* alleles (*gm107* and *gm108*) were identified.

Several results suggest that mutations causing the strongest phenotypes represent null alleles. First, homozygous (*vab-8(strong)/vab-8(strong)*) and hemizygous (*vab-8(strong)/Df)* animals exhibited Unc, Wit, Muv, Con, and ALA and AVKR axon outgrowth defects at similar penetrances and severities (see Results for description of types of *vab-8* alleles; Table 2; B.W. and G.G., unpublished data). Second, a strong *vab-8* allele behaved similarly to a deficiency when placed in *trans* to a weak *vab-8* allele. That is, heterozygous *vab-8(gm84)/vab-8(ct33)* and hemizygous *vab-8(gm84)/ctDf1* animals exhibited Unc, Wit, Pvl, Muv and Con defects at similar penetrances and severities (Table 2). Third, three of the *vab-8* alleles, one (*ct33*) isolated in a previous study and two (*gm107* and *gm108*) isolated in this study, were isolated in screens for mutations that failed to complement *vab-8(e1017)* or *vab-8(ct33)*. Because hemizygous *vab-8(e1017)/ctDf1* and *vab-8(ct33)/ctDf1* animals are viable, null alleles could have been isolated in these screens, even if null alleles of *vab-8* are lethal or sterile. In these screens no alleles were identified with more severe phenotypes than existing strong alleles. Finally, *vab-8* alleles were isolated at frequencies typical for mutations that reduce or eliminate gene function (Brenner, 1974; Greenwald and Horvitz, 1980). In two separate screens, one for alleles that fail to complement *vab-8(ct33)* (see above) and one for CAN-migration mutants (W. C. F., F. Wolf and G. G., unpublished results), the forward mutation frequency was 3.8×10^{-4} and 1.9×10^{-4}/mutagenized chromosome, respectively.

Because *vab-8* mutant males cannot mate, we were unable to establish homozygous *vab-8* mutant strains that produce the large number of males required for analysis of the CPn axons. *vab-8* mutant males were obtained by crossing the *vab-8* alleles into a *him-6(e1423)* mutant background, which causes a high incidence of males. Homozygous *him-6(e1423)* males were crossed to homozygous *vab-8* mutant hermaphrodites. F_1 wild-type progeny were obtained and numerous F_2 Vab-8 mutant progeny were picked to individual plates. F_2 animals that were also homozygous for *him-6(e1423)* were identified by the appearance of males in the F_3 generation.

Indirect immunofluorescence histochemistry and microscopy

Animals were raised at 25°C prior to fixation in all staining protocols. Animals were fixed, permeabilized and incubated with rabbit anti-serotonin or anti-GABA antisera (provided by J. Steinbusch, Free University, Amsterdam) as described by McIntire et al. (1992).

Fixation, permeabilization and incubation of animals with a rabbit anti-FMRF antiserum (provided by Chris Li, Boston University, Boston, MA) and rabbit anti-β-galactosidase antiserum (Promega) was performed by the same methods used for anti-serotonin staining.

For UNC-86 and 611B1 staining, animals were fixed, permeabilized and incubated with 1% UNC-86 antiserum (provided by M. Finney and G. Ruvkun, Massachusetts General Hospital, Boston, MA) or 0.5% monoclonal antibody 611B1 (provided by G. Piperno, Rockefeller University, New York, NY), as described by Finney and Ruvkun (1990). Occasionally animals were not permeabilized using this procedure. In these cases the animals were placed in a Dounce homogenizer and permeabilized with three strokes of the pestle. After the final wash, 5 μl of stained worms were mixed with 5 μl of a solution containing 20 mg/ml n-propyl gallate, 70% glycerol, 30 mM Tris-HCl, pH 9.5.

ADE and PDE are dopaminergic neurons. To visualize the axons of these neurons, we indirectly detected the activity of aromatic amino acid decarboxylase (Loer and Kenyon, 1993), the enzyme that synthesizes dopamine and serotonin from dopa and 5-hydroxytryptophan, respectively. 250 μl of a solution containing 20 mg/ml 5-hydroxytryptophan (Sigma) in M9 was added to a single 60 mm plate containing a growing population of nematodes, and the animals were incubated for 4 hours to overnight at 25°C. After the 5-hydroxytryptophan treatment, the animals were fixed, permeabilized and stained with anti-serotonin antiserum as described by McIntire et al. (1992). Dopaminergic neurons take up the exogenously supplied 5-hydroxytryptophan, and because they contain aromatic amino acid decarboxylase, these cells synthesize serotonin from 5-hydroxytryptophan.

Stained worms were viewed by immunofluorescence microscopy using a Zeiss microscope and Zeiss filters no. 487910 and no. 487915. FITC- or Texas Red-conjugated secondary antibodies were obtained from Cappel, Inc. Images were photographed using Ektachrome T160 film, scanned with a Nikon scanner to a computer graphics file, and annotated and enhanced to improve contrast using the Adobe Photoshop graphics program.

glr-1::GFP, glr-1::mec-4(dm), ceh-23::lacZ and UL64A1 transgenic strains

To visualize the AVA, AVB, AVD and PVC neurons, we expressed an UNC-76-GFP fusion protein under the control of the *glr-1* promoter. The *glr-1* gene encodes a *C. elegans* glutamate receptor subunit, which is expressed in AVA, AVB, AVD, PVC and additional neurons. A complete description of the *glr-1::unc-76::GFP* strain is given by Maricq et al. (1995). Briefly, a hybrid gene containing the coding region for the first 197 amino acids of the UNC-76 protein (L. Bloom and H. R. Horvitz, personal communication) and the green fluorescent protein (GFP) of the jellyfish *Aequorea victoria* (Chalfie et al., 1994) was placed under the control of the *glr-1* promoter. Animals carrying a *glr-1::unc-76::GFP* extrachromosomal array were produced by germline transformation of *lin-15* animals with *lin-15* and *glr-1::unc-76::GFP* DNA (Mello et al., 1991). We treated these animals with γ-irradiation to yield a strain that possessed the *glr-1::unc-76::GFP* gene integrated into the genome. The fusion of the N-terminal region of *unc-76* to β-galactosidase had been shown to enhance the expression of β-galactosidase within axons and to exclude it from the nucleus (L. Bloom and H.R. Horvitz, personal communication). We observed a similar result using the *glr-1::unc-76::GFP* fusion protein (hereafter referred to as *glr-1::GFP*).

We used a *glr-1::mec-4(dm)* fusion gene to kill the AVA, AVB, and AVD neurons (see Results). This construct utilizes the same *glr-1* promoter described above, but fuses it to the cytotoxic *mec-4(dm)* gene (Driscoll and Chalfie, 1991). The details of the *glr-1::mec-4(dm)* fusion gene are described in Maricq et al. (1995).

We used a *ceh-23::lacZ* transgene to visualize the CAN axons. This construct is a translation fusion of the promoter and N-terminal region of *ceh-23*, which encodes a homeobox gene (Wang et al., 1993), to the 197 amino acid fragment of *unc-76* described above and the *lacZ* gene of *E. coli* (J. Zallen and C. I. B., unpublished data).

The UL64A1 transgene allowed the visualization of the excretory canals by β-galactosidase staining. This transgene is the UL6 line described by Young and Hope (1993).

In all cases the transgenes were crossed into *vab-8* mutant backgrounds by mating wild-type males to hermaphrodites that bore the transgene, and crossing F_1 males to homozygous *vab-8* hermaphrodites. Wild-type cross progeny were isolated and picked individually to single plates. Multiple F_2 *vab-8* progeny were picked individually to single plates and screened for the presence of the transgene by direct examination for fluorescence or β-galactosidase activity.

Analysis of PHA and PHB axon outgrowth requirements

PHA and PHB are sensory neurons in the tail that have shortened axons in *vab-8* mutants. To examine whether interneurons that express *glr-1* are required for normal PHA and PHB axon outgrowth, we used a strain that contained a *glr-1::mec-4(dm)* extrachromosomal array (*kyEx53*), which killed the *glr-1*-expressing cells. This strain also carried the integrated *glr-1::GFP* transgene (*kyIn29*), which allowed for the identification of the *glr-1*-expressing cells that were not killed by the array (Maricq et al., 1995). By epifluorescence microscopy, we identified animals that expressed the *glr-1::GFP* transgene in particular neurons and scored the PHA and PHB axons by filling with the fluorescent dye 3,3′-dioctadecyloxacarbocyanine (DiO; Molecular Probes) using a modification of the procedure developed by Hedgecock et al. (1985).

Scoring of axons and cells

Axons were scored as defective in Table 1 if they failed to reach their normal destination as defined by electron microscopic reconstructions of the *C. elegans* nervous system (White et al., 1986). Occasionally, in wild-type animals (or, in the case of the CPn axons, in *him-6(e1423)* animals) axons failed to reach their defined normal destination. This background of variability is shown in the wild-type column of Table 1. The extent of cell migration in wild-type and mutant animals was determined by comparing the positions of migratory cell bodies relative to the positions of non-migratory hypodermal cell bodies (see Fig. 8). In Table 1, for each migratory cell the region between hypodermal cells in which most of the cells were located in wild-type animals was defined as the normal destination. Cell bodies that were located in other regions along their normal route were scored as defective for migration. Thus, the wild-type column in Table 1 represents the natural variability of the position of a given cell. The data shown in Table 1 and Fig. 8 are for three representative alleles. The other *vab-8* alleles were scored for the following phenotypes and found to be similar to the corresponding representative allele: *gm107* and *gm108* were scored for AVA, AVB, AVD, AVKR, ALA, RID axons and all cell migrations described in Table 1; *ct33* and *rh205* were scored for ADE, AVA, AVB, AVD, AVKR, ALA, CPn, HSN, PDE, PVC, RID, RMG axons and all cell migrations described in Table 1; and *gm99* was scored for AVKR, ALA, RID axons and all cell migrations described in Table 1.

RESULTS

vab-8 mutations cause the premature termination of posteriorly directed axons

In *vab-8* mutants, we observed defects in four classes of neurons that extend axons posteriorly along the ventral nerve cord from cell bodies located in the head. The AVAs, AVBs, AVDs and AVKs are pairs of bilaterally symmetrical interneurons located near the nerve ring (Figs 2, 3). Each neuron extends a single axon partially around the nerve ring and then

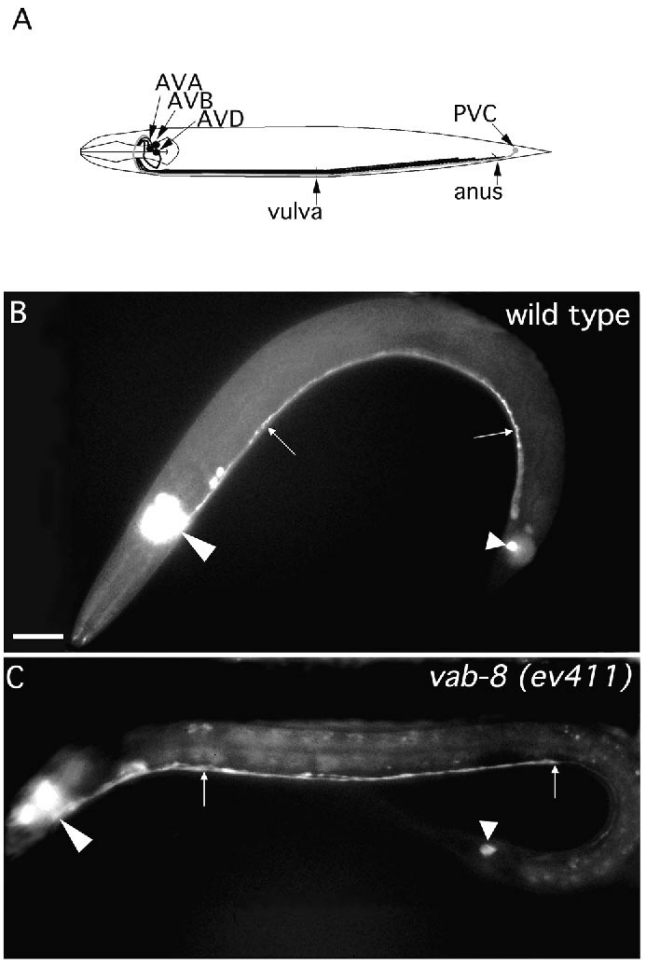

Fig. 2. AVA, AVB, AVD and PVC axon morphologies in wild-type and *vab-8* larvae. Anterior is to the left, dorsal at top. (A) Schematic drawing (lateral view) of a adult hermaphrodite showing the AVA, AVB, AVD and PVC axon morphologies. (B-C) Lateral view fluorescence photomicrographs of wild-type (B) and *vab-8(ev411)* (C) larvae containing an integrated *glr-1::GFP* transgene that expresses GFP in AVA, AVB, AVD, PVC and other neurons. The AVA, AVB, AVD and PVC axons (arrows) extend along the ventral nerve cord. AVA, AVB and AVD extend axons posteriorly from cell bodies (large arrowheads) located in the head, and PVC extends an axon anteriorly from its cell body in the tail (small arrowheads). The arrows indicate two similar longitudinal positions in both B and C. Note the termination of the AVA/AVB/AVD axon bundle at the right arrow in C. Scale bar, 20 μm.

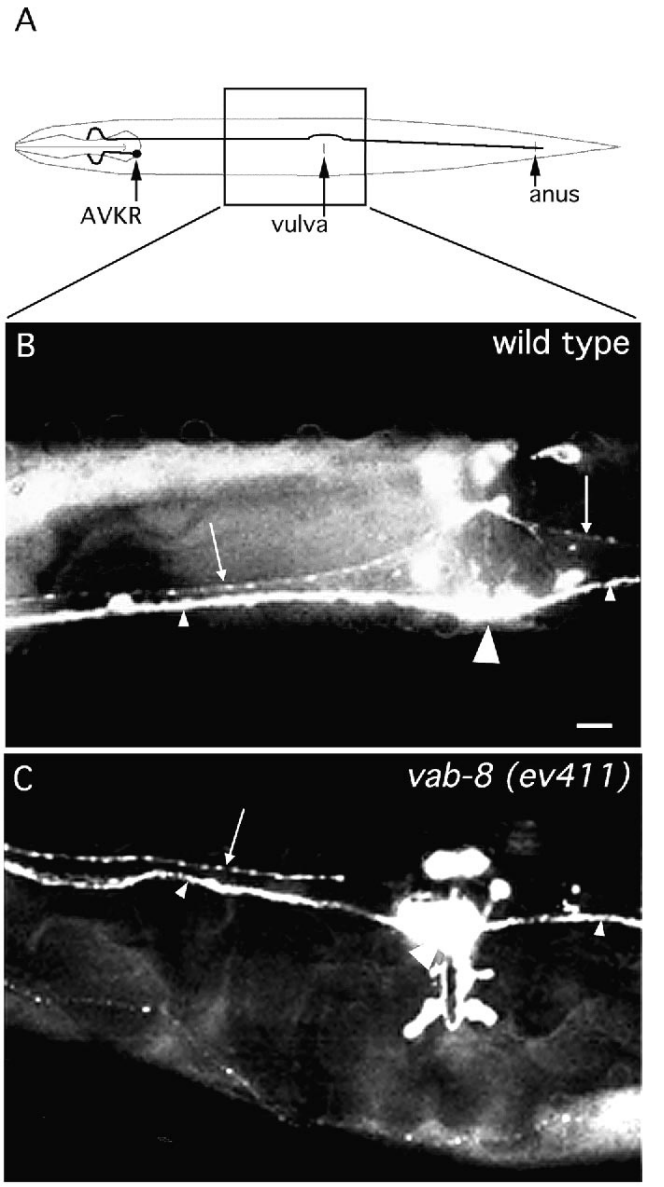

Fig. 3. AVKR axon morphology in wild-type and *vab-8* hermaphrodites. Anterior is to the left, ventral view. (A) Schematic drawing (ventral view) of a wild-type adult hermaphrodite showing AVKR axon morphology. The boxed area is the portion of the animal shown in B and C. (B,C) Immunofluorescence photomicrographs of wild-type and *vab-8(ev411)* adult hermaphrodites stained with an anti-FMRFamide antiserum to detect the AVKR axon. (B) Oblique ventral view of a wild-type adult hermaphrodite. The AVKR axon (arrows) extends along the left bundle of the ventral nerve cord. It can be distinguished from other axons that stain with the anti-FMRFamide antiserum because AVKR is the only intensely staining axon that extends along the left bundle of the ventral nerve cord. The small arrowheads mark the FMRFamide immunoreactive axons of the right ventral nerve cord bundle. The large arrowhead marks the position of the vulva where additional cells in this region also stain with anti-FMRFamide antiserum. (C) Oblique ventral view of a *vab-8(ev411)* adult hermaphrodite. The AVKR axon (arrow) terminates prematurely, anterior to the vulva (large arrowhead). Scale bar, 10 μm.

posteriorly along the ventral nerve cord to the tail (White et al., 1976, 1986).

The AVA, AVB and AVD axons can be visualized in a *glr-1::GFP* transgenic strain (Maricq et al., 1995; see Materials and Methods) and one AVK axon, AVKR, can be detected using an anti-FMRFamide antiserum (Schinkmann and Li, 1992). In *vab-8* mutants, the cell bodies of these neurons occupied their normal positions, but their axons terminated prematurely, ending in the ventral nerve cord at positions roughly midway between the nerve ring and the anus (Figs 2C, 3C; Table 1). Therefore, *vab-8* is required for these axons to extend to their normal length.

The six male-specific CP neurons are located in the ventral

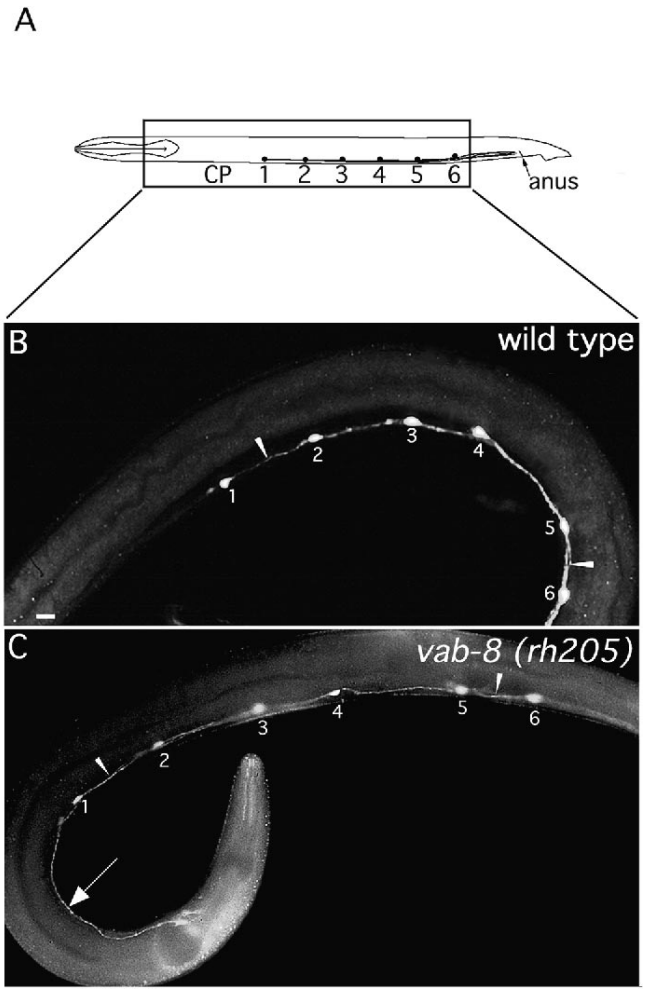

Fig. 4. CPn axon morphology in wild-type and *him-6; vab-8* males. Anterior is to the left, dorsal at top. CP1-CP6 cell bodies are numbered. (A) Schematic drawing (lateral view) of a wild-type adult male showing CPn axon morphology. CPn axon morphology is the same in *him-6* and wild-type males. The boxed area is the portion of the animals shown in B and C. (B,C) Immunofluorescence photomicrographs of wild-type and *him-6(e1423); vab-8(rh205)* adult males that were stained with an anti-serotonin antiserum to detect the CP1-CP6 axons. Arrowheads point to the CPn axons in the right bundle of the ventral nerve cord. (B) Lateral view of a wild-type adult male. CP1-CP6 extend axons posteriorly along the right bundle of the ventral nerve cord. (C) Lateral view of a *him-6; vab-8(rh205)* adult male. Axons that extend anteriorly of CP1 are indicated by the arrow. Scale bar,10 μm.

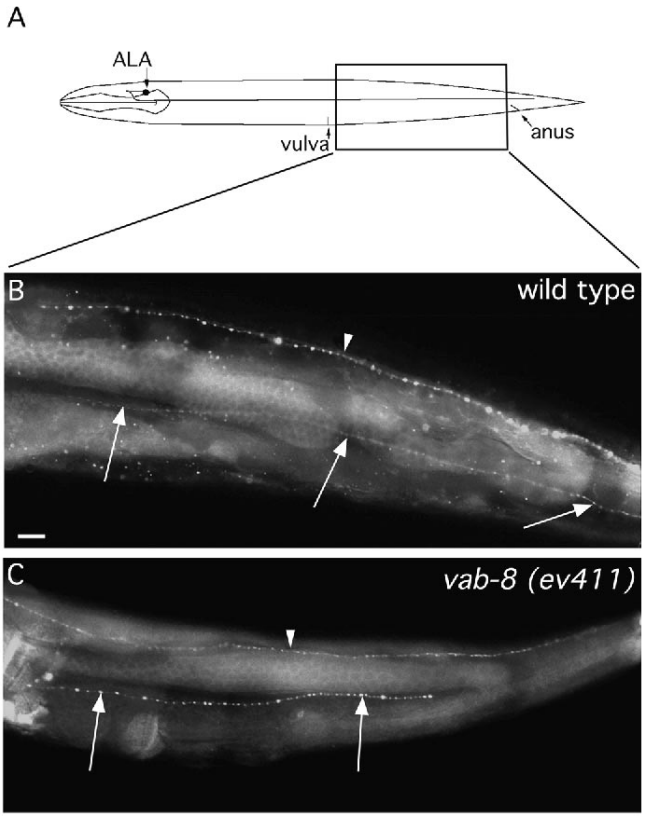

Fig. 5. ALA axon morphology in wild-type and *vab-8* hermaphrodites. Anterior is to the left, dorsal at the top. (A) Schematic drawing (left lateral view) of a wild-type adult hermaphrodite showing ALA axon morphology on the left side. ALA also extends a similar lateral process on the right side (not shown). The boxed area is the portion of the animal shown in B and C. (B,C) Immunofluorescence photomicrographs of wild-type and *vab-8(ev411)* adult hermaphrodites that were stained with an anti-FMRFamide antiserum to reveal ALA (arrows) and RID (arrowhead) axon morphology. (B) Left lateral view of a wild-type adult hermaphrodite. The ALA axon extends posteriorly to the tail along the lateral body wall. The RID axon can also be seen extending posteriorly to the tail along the dorsal nerve cord. (C) Left lateral view of a *vab-8(ev411)* adult hermaphrodite. The ALA axon stops prematurely before reaching the tail. As in wild type, the RID axon extends posteriorly to the tail. Scale bar, 10 μm.

cord along the midbody and each extends an axon posteriorly along the ventral nerve cord to the diagonal muscles located in the posterior half of the body (Sulston et al., 1980; Fig. 4). The anatomy of the CPn axons was examined using anti-serotonin antibodies (Loer and Kenyon, 1993). In wild-type males, the CP axons extended posteriorly in a bundle that thickened near the tail as more CP axons were added. By contrast, in *vab-8* males, the diameter of the CP axon bundle near the tail was thinner than in wild-type males, suggesting that some CP axons failed to reach their normal destinations (data not shown). In addition, CPn axons often projected anteriorly beyond the CP1 cell body in *vab-8* mutants, implying that some CPn growth cones extended anteriorly rather than posteriorly from a CPn cell body (Fig. 4C; Table 1).

ALA is a single interneuron located in the head that extends two bilaterally symmetrical processes along lateral nerve bundles to the tail (White et al., 1986 and Fig. 5A). Immunofluorescent staining of animals with an anti-FMRFamide antiserum revealed that the ALA axons failed to reach the tail in *vab-8* mutants (Fig. 5C; Table 1). Thus, *vab-8* is required for the posteriorly directed outgrowth of axons in the ventral nerve cord and in a lateral nerve cord.

We identified one posteriorly directed axon unaffected by *vab-8* mutations. RID is a single motorneuron that extends several axons, the longest of which extends along the dorsal cord to the tail (White et al., 1986). Using an anti-FMRFamide antiserum, we observed no defects in RID axon morphology in *vab-8* mutants (Fig. 5C; Table 1). Thus, the posteriorly

directed outgrowth of eight of nine classes of axons examined depend upon *vab-8* function.

Most anteriorly directed and circumferential axons are normal in *vab-8* mutants

We also examined anteriorly directed axon outgrowth in *vab-8* animals. The PVC interneurons, which can be visualized in the *glr-1::GFP* strain, are located in the tail and extend axons along the ventral nerve cord to the nerve ring (Fig. 2). The HSN motorneurons, which can be detected using an anti-serotonin antiserum, are located in the midbody and extend axons ventrally to the ventral nerve cord and then anteriorly to the nerve ring. The ALMs and PLMs are each symmetric pairs of sensory neurons that can be detected using an anti-tubulin monoclonal antibody. The ALMs are located in the midbody and extend lateral axons anteriorly to the nerve ring, while the PLMs are positioned in the tail and extend lateral axons anteriorly to the midbody (White et al., 1986, and Fig. 1). The anteriorly directed PVC, HSN, ALM and PLM axons were normal in *vab-8* mutants (Table 1).

Circumferential growth cone migrations were also unperturbed in *vab-8* mutants. The ventral migrations of ADE, HSN, RMG, and PDE growth cones and the dorsal migrations of the DDn and VDn motor neuron growth cones were all normal in *vab-8* animals (Table 1).

vab-8 mutations preferentially disrupt outgrowth of posteriorly directed axons of two bipolar neurons

In principle, *vab-8* could function in both anteriorly and posteriorly directed growth cone migrations in a subset of neurons. A general function of *vab-8* in migration may not be reflected in our data if the neurons we sampled were fortuitously biased towards neurons with posteriorly directed axons that require *vab-8* and anteriorly directed and circumferential axons that do not require *vab-8*. Evidence that *vab-8* is specifically required for posteriorly directed migrations was provided by examining the PDE and CAN neurons, each of which extend both an anteriorly and a posteriorly directed axon. The PDEs are a pair of bilaterally symmetrical dopaminergic mechanosensory neurons located laterally in the posterior body (Fig. 6A). Each PDE neuron extends an axon to the right ventral nerve cord, where it bifurcates and extends one axon anteriorly to a position behind the pharynx and a second axon posteriorly to a position near the anus (White et al., 1986 and Fig. 6).

Table 1. Axon outgrowth and cell migration defects in *vab-8* mutants

Cell/Axon[b]	Method of detection[c]	Percentage defective (*n*)[a]			
		wild type	*e1017*	*gm84*	*ev411*
Posteriorly directed axons					
ALA	FMRF	0 (47)	96 (26)	68 (22)	96 (24)
AVA, AVB, AVD[d,e]	*glr-1::GFP*	0 (30)	100 (70)	100 (60)	100 (85)
AVKR	FMRF	4 (27)	97 (30)	88 (25)	97 (39)
CAN[e,f]	*ceh-23::lacZ*	0 (21)	100 (19)	76 (25)	89 (25)
CPn[g]	serotonin	5 (22)	66 (29)	39 (23)	80 (20)
PDE	AADC	5 (22)	66 (35)	31 (26)	78 (54)
RID	FMRF	0 (28)	0 (22)	0 (22)	0 (21)
Posteriorly directed cells					
ALM	DIC	2 (50)	31 (54)	36 (50)	40 (50)
CAN	DIC	0 (50)	98 (51)	78 (50)	0 (53)
ccmL	DIC	8 (50)	98 (54)	96 (50)	31 (52)
ccmR[h]	DIC	4 (50)	44 (52)	20 (50)	8 (50)
M	DIC	5 (25)	0 (25)	0 (26)	0 (25)
PQR	DIC/UNC-86	0 (25)	32 (28)	20 (15)	32 (28)
Z1/Z4	DIC	0 (50)	0 (50)	0 (50)	0 (50)
Posteriorly directed process					
excretory canal[e]	UL64A1	0 (13)	90 (20)	80 (20)	74 (42)
Anteriorly directed axons					
ALM	α-tubulin	0 (28)	0 (20)	0 (25)	0 (22)
CAN[e]	*ceh-23::lacZ*	0 (21)	N.A.[k]	N.A.[k]	0 (26)
HSN	serotonin	0 (50)	0 (40)	0 (24)	0 (24)
PDE	AADC	0 (19)	0 (23)	0 (23)	0 (26)
PHA,PHB[d]	diO	6 (31)	N.D.[l]	64 (25)	74 (23)
PLM	α-tubulin	0 (23)	0 (20)	0 (24)	0 (13)
PVC[e,i]	*glr-1::GFP*	0 (24)	0 (22)	N.D.	N.D.
Anteriorly directed cells[j]					
HSN	DIC	2 (50)	3 (58)	6 (50)	0 (50)
QR	DIC/UNC-86	0 (20)	0 (15)	0 (15)	0 (10)
Ventrally directed axons					
ADE	AADC	0 (22)	0 (35)	0 (20)	0 (54)
HSN	serotonin	0 (50)	7 (38)	8 (52)	0 (24)
RMG	FMRF	0 (32)	0 (28)	5 (21)	0 (26)
PDE	AADC	0 (44)	0 (70)	0 (52)	0 (98)
Dorsally directed cells and axons					
dtc	DIC	0 (20)	0 (25)	0 (10)	0 (25)
DDn	GABA	0 (300)	0 (168)	0 (168)	0 (144)
VDn	GABA	0 (650)	0 (284)	0 (260)	0 (52)

We examined PDE axon morphology using an immunocytochemical technique that detects aromatic amino acid decarboxylase activity (see Materials and Methods). In wild-type and *vab-8* animals, the PDEs extended axons to the ventral nerve cord, and the anteriorly directed axons of the PDEs reached their normal positions behind the pharynx. However, the posteriorly directed PDE axons were shortened or missing in *vab-8* mutants (Fig. 6C; Table 1).

The CANs are a pair of bilaterally symmetrical neurons located near the center of the animal (Fig. 7). Each CAN extends one axon anteriorly to the nerve ring and a second axon posteriorly to the tail, both along a lateral nerve bundle (White et al., 1986; Durbin, 1987). We examined CAN axon morphology in animals bearing a *ceh-23::lacZ* transgene (J. Zallen and C. I. B., unpublished results). In *vab-8(ev411)* and *vab-8(gm107)* animals (see below for discussion of different *vab-8* alleles), the CAN cell bodies were found in their normal positions, and the anterior CAN axons extended normally to the nerve ring. However, the posteriorly directed CAN axons terminated prematurely (Fig. 7C; Table 1). In other *vab-8* mutants (*ct33*, *gm84*, *gm99*, *gm108*, *e1017*, and *rh205*), the posteriorly directed CAN axons also terminated before reaching their normal destination in the tail. However, these *vab-8* mutations also disrupted CAN cell migration (Fig. 7D, and see below). Therefore, anterior displacement of the CAN cell body may contribute to the severity of the CAN axon defect in these mutants.

These data show that for two cell types, *vab-8* mutations disrupt posteriorly directed growth cone migrations, but have no effect on migrations in other directions.

vab-8 mutations and ventral cord lesions cause PHA and PHB axon outgrowth defects

The PHAs and PHBs are bilaterally symmetrical bipolar sensory neurons located in the tail. Each PHA and PHB neuron extends an axon ventrally and then anteriorly along the ventral nerve cord. PHA and PHB can be visualized by staining with the vital dye DiO (Hedgecock et al., 1985; see Materials and Methods). In *vab-8* mutants, the anteriorly directed axons of PHA and PHB were often shorter than in wild type (Table 1; J. Culotti, personal communication).

A similar PHA and PHB outgrowth defect can be caused by killing other ventral cord neurons. In a *glr-1::mec-4 (dm)* transgenic strain (Maricq et al., 1995), many neurons, including AVA, AVB, AVD, PVC and PVQ, degenerate because of the expression of the toxic MEC-4 degenerin protein (Driscoll and Chalfie, 1991). We found that the PHA and PHB axons stopped prematurely in *glr-1::mec-4(dm)* animals, a phenotype like that seen in *vab-8* mutants. Because the *glr-1::mec-4(dm)* transgene is not expressed in PHA and PHB (Maricq et al., 1995), these results indicate that defects in PHA and PHB axon outgrowth can be caused by defects in other neurons.

To determine which *glr-1::mec-4(dm)*-expressing neurons were needed for normal PHA and PHB axon extension, we iden-

Table 1. Footnotes

[a]Percentage of cells or axons that failed to migrate or extend to wild-type positions. The data for wild type (N2) and a strong (*e1017*), weak (*gm84*) and Unc (*ev411*) *vab-8* mutants are reported. Similar results were observed for other *vab-8* mutants of each class (see Materials and Methods). *n*, the number of cells or axons analyzed.

[b]See Materials and Methods for description of cell and axon identification.

[c]Method used to examine the cell position or axon morphology: FMRF, immunocytochemical staining with an anti-FMRFamide antiserum (Marder et al., 1987; Schinkmann and Li, 1992); *glr-1::GFP*, epifluorescence of transgenic strain expressing GFP (Green Fluorescent Protein) from the *glr-1* promoter (Maricq et al., 1995); *ceh-23::lacZ*, immunocytochemical staining using anti-β-galactosidase antiserum to detect β-galactosidase expressed from the *ceh-23* promoter (J. Zallen and C. I. B., unpublished results); serotonin, immunocytochemical staining with an anti-serotonin antiserum (Garriga et al., 1993); AADC, immunocytochemical staining with an anti-serotonin antiserum of animals grown in 5-hydroxytryptophan to detect aromatic amino acid decarboxylase in dopaminergic neurons (Loer and Kenyon, 1993); UL64A1, β-galactosidase immunocytochemical staining of animals bearing an integrated promoter trap transgene expressed in the excretory cell (derived from line UL6, Young and Hope, 1993); DIC, Nomarski differential interference contrast microscopy; UNC-86, immunocytochemical staining with an anti-UNC-86 antiserum (Finney and Ruvkun, 1990); α-tubulin, immunocytochemical staining with the anti-acetylated-α-tubulin monoclonal antibody 611B1 (Piperno and Fuller, 1985; Siddiqui et al., 1989); DiO, epifluorescence of animals after soaking in the lipophilic dye DiO (Hedgecock et al., 1985); GABA, immunocytochemical staining with an anti-GABA antiserum (McIntire et al., 1992).

[d]These axons extend together in a bundle; we scored the axons as normal if any extended to the wild-type length.

[e]For *glr-1::GFP*, *ceh-23::lacZ* and UL64A1, 'wild type' indicates the phenotype of animals that carry the transgene, but no *vab-8* mutation.

[f]The posteriorly directed axon outgrowth defects of CAN for *e1017* and *gm84* were more severe than those for *ev411*. In *e1017* and *gm84* mutants, the CAN cells were often anterior to the nerve ring; in such cases, the posteriorly directed axons typically failed to extend out of the head and occasionally entered the nerve ring.

[g]CPn axons were analyzed in *him-6(e1423)* (high incidence of males) males (wild type) or in *him-6; vab-8* double mutant males. Similar results were observed for rare, spontaneous *vab-8* males. Individual CPn axons could not be scored because the CPn axons extend along the ventral nerve cord as a single bundle. Animals were scored as defective if axons extended anteriorly of CP1 (Fig. 4). Some animals that did not have CPn axons extending anteriorly of CP1, displayed thinning of the CPn axon bundle in the posterior portion of the animal, suggesting that some axons were not reaching their normal posterior destinations. However, for the purposes of this table these animals were not counted as defective.

[h]We observed subtle defects in the migrations of ccmR (Fig. 8) that were not reported by Manser and Wood (1990).

[i]The PVC axons extend from the tail to the nerve ring along the ventral nerve cord. The presence of other axons in the ventral nerve cord that express the *glr-1::GFP* transgene (i.e. AVA, AVB and AVD) prevented the unique identification of the PVC axons in *glr-1::GFP* animals. To score these axons in a non-*vab-8* background, we constructed a *glr-1::GFP* strain that contained an *glr-1::mec-4(dm)* extrachromosomal array (see text) and identified animals that had one or both PVC axons but lacked most or all of the *glr-1::GFP*-positive axons that extended posteriorly along the ventral nerve cord. The 'wild-type' data indicates the number of mosaic animals in which PVC axons were found to extend the complete length of the ventral cord. To determine PVC axon outgrowth in a *vab-8(e1017)* mutant background, we scored the PVC axons only in animals in which the posteriorly directed axons (i.e. AVA, AVB, and AVD) stopped shortly after entering the ventral nerve cord. In these animals, the PVC axons could be seen to extend the length of the ventral nerve cord. Similar results were obtained with other strong *vab-8* mutations (*ct33*, *rh205*). We could not determine the lengths of the PVC axons in the other *vab-8* alleles because the posteriorly directed axons typically extended to the midbody region.

[j]The HSN and QR descendants were occasionally slightly anterior of their normal positions in *vab-8* mutants (see Fig. 8 and results). These excessive migrations were not reported as defective in this table.

[k]N. A., not applicable. The anterior-directed axon of CAN normally enters the nerve ring. In strong and weak *vab-8* mutants, the CAN neuron is often anterior to the nerve ring, and the anterior axon extends to the nose. When the CAN neuron is posterior to the nerve ring, the anterior CAN axon extends to the nerve ring.

[l]N. D., not determined. In strong *vab-8* mutants such as *e1017*, the PHA and PHB neurons failed to fill with DiO.

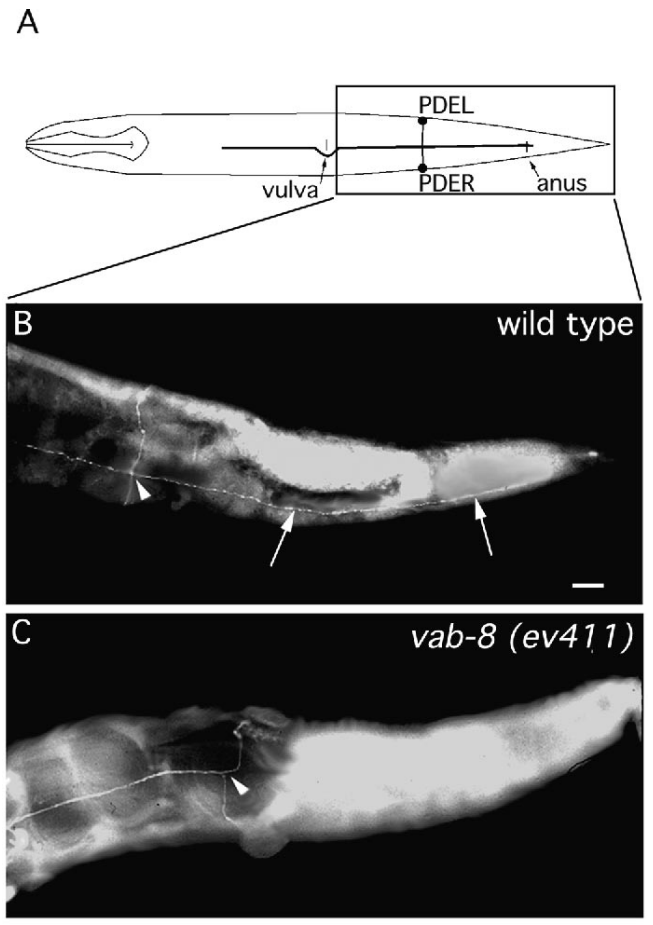

Fig. 6. PDE axon morphology in wild-type and *vab-8* hermaphrodites. Anterior is to the left, ventral view. (A) Schematic drawing (ventral view) of a wild-type adult hermaphrodite showing PDE axon morphology. The positions of the PDEL and PDER cell bodies are shown as closed circles. Arrows show the location of the vulva and anus. The boxed area is the portion of the animal shown in B and C. (B,C) Immunofluorescence photomicrographs of wild-type and *vab-8(ev411)* adult hermaphrodites that were incubated in 5-hydroxytryptophan, fixed and stained with an anti-serotonin antiserum to reveal PDE axon morphology (see Materials and Methods). (B) Oblique ventral view of a wild-type adult hermaphrodite. The PDE axons extend ventrally and enter the right bundle of the ventral nerve cord. In the ventral nerve cord, the axons bifurcate (arrowhead). Each PDE extends an axon anteriorly and an axon posteriorly (arrows) along the ventral nerve cord. (C) Ventral view of a *vab-8(ev411)* adult hermaphrodite. No PDE axons are detected in the ventral nerve cord posterior to the position where the axons enter the ventral nerve cord (arrowhead). Scale bar, 10 μm.

tified animals that retained a subset of *glr-1*-expressing neurons (see Materials and Methods). We identified nine animals that lacked AVA, AVB and AVD and retained one PVC (two animals), one PVQ (four animals), or one PVC and one PVQ (three animals). All nine animals had shortened PHA and PHB axons. These results suggest that normal PHA and PHB axon outgrowth depends on axons that extend from the head to the tail. Therefore, defects in the outgrowth of AVA, AVB, and/or AVD axons, which normally overlap the PHA/PHB axons in the preanal ganglion, might lead to the premature termination of the PHA and PHB axons in *vab-8* mutants.

vab-8 mutations disrupt posteriorly directed cell migrations

Manser and Wood (1990) reported that two *vab-8* mutations, *e1017* and *ct33*, disrupt the migrations of the ALM and CAN neurons and the coelomocyte mother cell, ccmL. We examined the positions of eight cell types that migrate posteriorly: the neurons CAN and ALM, the progeny of the left and right coelomocyte mother cells (ccmL and ccmR), the mesoblast M, and the somatic gonad precursors Z1 and Z4, which all migrate during embryonic development, and the PQR neurons, which migrate during larval development (Sulston and Horvitz, 1977; Kimble and Hirsh, 1979; Sulston et al., 1983; Hedgecock et al., 1987). To determine the positions of these cells in wild-type and in *vab-8* mutants, we observed the cells directly by Nomarski differential interference contrast microscopy. In strong *vab-8* mutants, we often found the cell bodies of ALM, CAN, ccmL, ccmR and PQR in positions anterior to their normal location, suggesting that *vab-8* activity is needed for these posteriorly directed cell migrations (Fig. 8; Table 1). By contrast, none of the *vab-8* mutations caused defects in the positions of M, Z1 and Z4, indicating that these cell migrations do not require *vab-8* function (Table 1; data not shown). The dorsal migrations of distal tip cells (dtc) of the gonad were also normal.

We also examined the morphology of the processes extended by the excretory cell. The excretory cell is located ventral to the posterior bulb of the pharynx and extends four tubular processes, called canals (Nelson and Riddle, 1984). In wild-type animals, two canals extend anteriorly and two canals extend posteriorly along the left and right lateral body wall past the anus (Nelson et al., 1983; Sulston et al., 1983; White et al., 1986). To examine the morphology of the excretory cell canals, we used a promoter-trap transgene (UL64A1) that expresses β-galactosidase in the canals (Young and Hope, 1993). In *vab-8* mutants, the posteriorly directed canals of the excretory cell terminated prematurely (Table 1).

Some anteriorly directed cell migrations occasionally overshoot their normal destinations in *vab-8* mutants

Most anteriorly directed cell migrations were normal or enhanced in *vab-8* mutants. The HSN cell bodies migrate anteriorly during embryonic development (Sulston et al., 1983). As reported previously (Manser and Wood, 1990), in some animals one or both HSNs migrated slightly anterior to their normal destinations (11/51 HSNs migrate beyond their normal destination in *vab-8(rh205)* mutants; Fig. 8; Table 1).

The neuroblast QL migrates posteriorly during postembryonic development, while its homolog QR and its descendants migrate a longer distance anteriorly (Sulston and Horvitz, 1977). As noted above, the posterior migration of the QL daughter PQR is shortened in *vab-8* mutants. By contrast, the QR daughters, AVM and SDQR, migrated to positions that were slightly anterior to their normal locations (5/14 for *vab-8(e1017)* mutants). These results suggest that like the HSNs, QR and its descendants occasionally migrate beyond their normal destinations in *vab-8* mutants.

vab-8 mutations do not alter cell fates along the longitudinal body axis

As in other animals, anteroposterior positional information in

C. elegans is conferred by a cluster of Hox (or homeotic) genes (Bürglin and Ruvkun, 1993; Wang et al., 1993). Cell fate determination of many stationary cell types as well as the position of some migrating cells is altered when the anteroposterior axis is shifted by mutations in the Hox genes. We examined the fates of several cell types along the longitudinal axis and found no alterations in anteroposterior patterning in *vab-8* mutants.

During postembryonic development, twelve Pn.a neuroblasts (P1.a-P12.a), which are located along the ventral cord, each divide to generate several types of neurons. The Pn.a precursors at different longitudinal positions produce different cell types; e.g. the centrally positioned neuroblasts (P3.a-P8.a) each produce a VC motor neuron, while the other Pn.a neuroblasts do not. In *vab-8* mutants, the VC neurons were centrally positioned as in wild type, suggesting that they were derived from P3.a-P8.a. Homologous neuroblasts in the male give rise to the CP neurons described above; the cell bodies of the CP neurons were also found in their correct positions in *vab-8* mutants.

Similarly, the twelve V cell precursors (V1L/R-V6L/R), located along the midlateral surface of the animal, undergo several rounds of division to generate epithelial cells and neurons. V5L and V5R, but not other V cells, produce the posterior deirid sensory organs. Each posterior deirid sensory organ was properly positioned in *vab-8* mutants, indicating that it was derived from V5 (data not shown). Thus, *vab-8* mutations do not alter the fates of the Pn.a and V cells along the longitudinal axis.

vab-8 mutants did display defects in some non-migrating cells, such as those involved in vulval development (Manser and Wood, 1990; Table 2). The strongest *vab-8* mutations caused two defects in vulval development: a protruding vulva (Pvl) and a multivulva phenotype (Muv) (Table 2). Unlike most Muv mutants (Ferguson et al., 1987), the ectopic vulval protrusions in *vab-8* mutants were always posterior to the vulva.

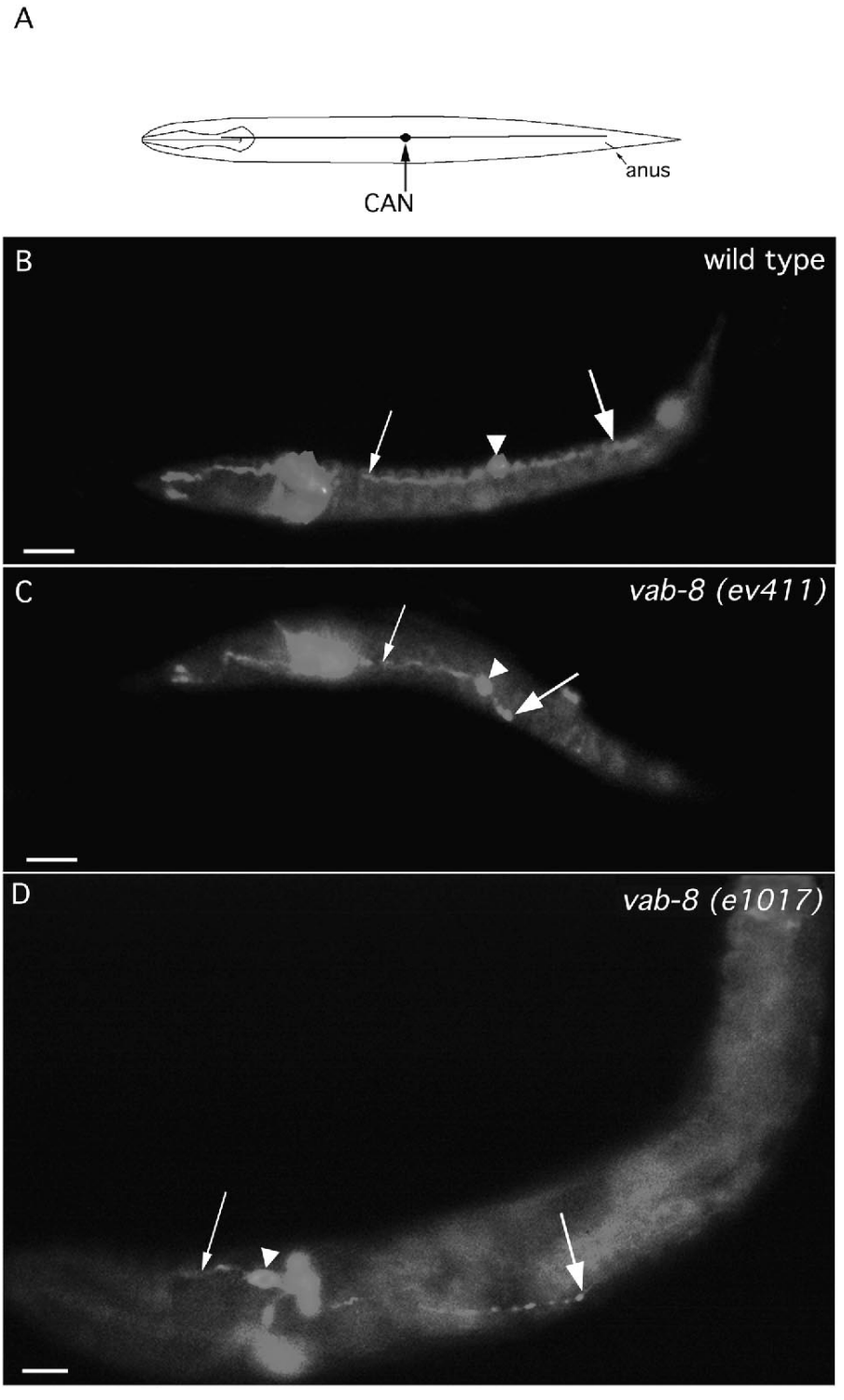

Fig. 7. CAN cell body position and axon morphology in wild-type and *vab-8* mutants. Anterior is to the left, dorsal at top. (A) Schematic drawing (lateral view) of a wild-type larva showing CAN cell body position and axon morphology. (B,C) Immunofluorescence photomicrographs of wild-type, *vab-8(ev411)* and *vab-8(e1017)* animals that contain the *ceh-23::lacZ* transgene and were stained with an anti-β-galactosidase antiserum. (B) Left lateral view of a wild-type L1 larva that bears the *ceh-23::lacZ* transgene. The CAN anteriorly directed axon (small arrow) and posteriorly directed axon (large arrow) emerge from the centrally positioned cell body (arrowhead). Additional neurons stain in the head and tail. (C) Left lateral view of a *vab-8(ev411)* L1 larva that bears the *ceh-23::lacZ* transgene. The cell body is properly positioned, but the posterior axon terminates prematurely at the position of the large arrow. (D) Left lateral view of a *vab-8(e1017)* L3 larva that bears the *ceh-23::lacZ* transgene. The cell body is mislocated just posterior to the pharynx, and the posterior axon terminates prematurely. Scale bars, 10 μm.

Table 2. *vab-8* mutant phenotypes[a]

Genotype[b]	% Unc	% Wit	% Pvl	% Muv	% Con	*n*[c]
Wild type	0	0	0	0	0	>100
Strong mutations						
vab-8(ct33)	98	79	36	5	17	42
vab-8(e1017)	100	79	33	17	12	57
vab-8(gm99)	100	81	43	11	11	37
vab-8(rh205)	100	94	49	30	17	53
Weak mutations						
vab-8(gm84)	79	21	10	4	4	52
vab-8(gm108)	97	39	30	11	11	37
Unc mutations						
vab-8(ev411)	100	0	0	0	0	53
vab-8(gm107)	100	0	0	0	0	30
Heteroallelic combinations						
vab-8(ev411)/ vab-8(ct33)	100	0	0	0	0	22
vab-8(ev411)/ctDf1	100	0	0	0	0	27
vab-8(gm84)/ vab-8(ct33)	97	61	33	8	14	36
vab-8(gm84)/ctDf1	97	66	42	18	13	38
vab-8(rh205)/ctDf1	100	93	81	26	11	27

[a]The penetrances of uncoordinated (Unc), withered tail (Wit), protruding vulva (Pvl), multivulva (Muv) and constipation (Con) phenotypes of wild type and *vab-8* mutants are reported, as scored by examination under the dissecting microscope . The Wit, Pvl and Muv phenotypes are described in detail by Manser and Wood (1990). Briefly, Unc animals have abnormal movement, Wit animals have a prominent shriveling of the posterior half of the body, Pvl animals have an everted bulge of tissue at the vulva, and Muv animals have additional vulva-like protrusions at positions posterior to the vulva. Animals that were pale in color, due to retention of material in the intestine, were scored as Con. Possibly due to differences in scoring, our results for some phenotypes of *vab-8(ct33)* and *vab-8(e1017)* differed slightly from Manser and Wood (1990).

[b]Genotypes of animals that were *vab-8* homozygotes, *vab-8* heteroallelic combinations or *vab-8* mutations in *trans* to *ctDf1*, a deficiency that deletes *vab-8* and neighboring loci.

[c]*n*, number of animals scored.

vab-8 encodes two genetic activities

All eight *vab-8* alleles characterized were recessive and behaved as loss-of-function mutations (Table 2). We grouped *vab-8* mutations into three classes based on behavioral and anatomical phenotypes: strong (*ct33, e1017, gm99, rh205*), weak (*gm84*, *gm108*), and uncoordinated or Unc (*ev411, gm107*).

Strong and weak *vab-8* mutants displayed Unc, Wit, Muv, Pvl and Con phenotypes (Table 1), as well as the axon outgrowth and cell migration defects described above (Table 2). The strong *vab-8* alleles behaved as genetic null alleles (see Materials and Methods) and therefore likely eliminate most or all *vab-8* activity. All phenotypes of the weak alleles were less severe than the strong alleles and were enhanced in *trans* to a deficiency (Table 1 and 2). Thus, the weak alleles appear to be partial loss-of-function alleles that retain some *vab-8* activity.

The Unc *vab-8* mutations caused defects in movement, axon outgrowth and some cell migrations comparable to strong mutations, but did not cause Wit, Pvl, Muv or Con phenotypes (Tables 1 and 2; data not shown). Moreover, Unc *vab-8* mutations did not affect CAN cell migration (Fig. 8; Table 1). Unlike the weak allele *gm84*, the phenotypes caused by *vab-8(ev411)* in *trans* to a deficiency were similar to *vab-8(ev411)* homozygotes (Table 2). Furthermore, *ev411/ctDf1* animals did not display Wit, Pvl or Muv phenotypes.

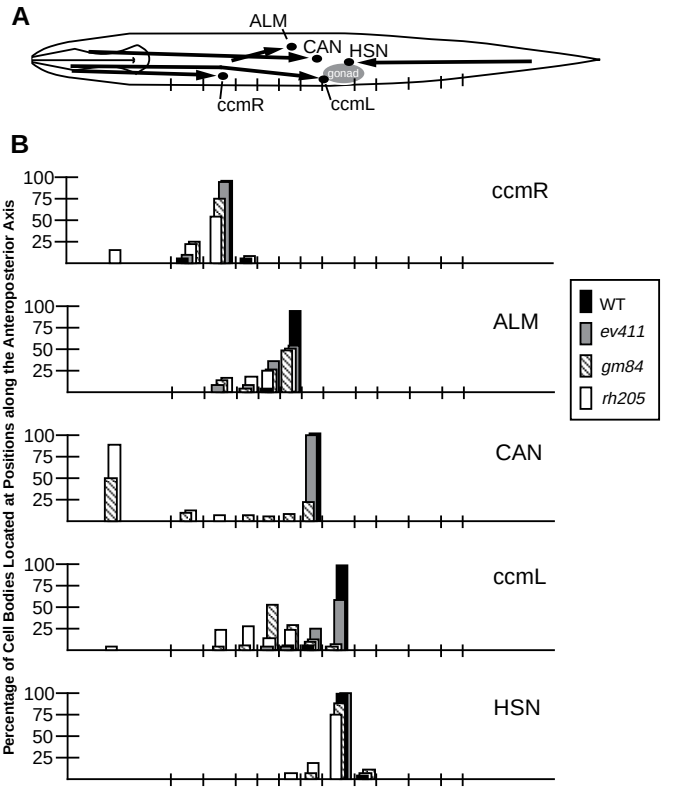

Fig. 8. Embryonic cell migration defects displayed by *vab-8* mutants. (A) Schematic diagram showing migration routes (indicated by arrows) of selected cells that undergo longitudinal migrations. These migrations occur during embryogenesis at times when the animal is shorter than in the first larval stage (L1) animals shown in the diagram. The positions of these cells were determined by Nomarski optics in newly hatched L1 larvae. The short vertical lines along the ventral side of the animal mark the positions of epithelial (hypodermal) nuclei that were used as landmarks to define the final positions of the migratory cells along the longitudinal axis. (B) The short vertical lines along the x axis in each graph correspond to the positions of the epithelial landmark nuclei in A. Positions of migratory cells in wild-type and a representative mutant for each *vab-8* mutant class (see text) are shown.

These results indicate that *vab-8* is a complex locus that encodes two genetic activities. Unc mutations eliminate one *vab-8* activity, which is required for a subset of migrations, while strong and weak mutations eliminate or reduce both *vab-8* activities.

DISCUSSION

Three observations indicate that *vab-8* acts in a global mechanism for directing posteriorly directed cell migration and axon outgrowth. First, *vab-8* mutations disrupted fourteen of the seventeen posteriorly directed axon and cell migrations examined, but only two of the seventeen circumferential and anteriorly directed axon and cell migrations examined. Second, *vab-8* mutations had selective effects on cells of similar type that differed only in their direction of migration. The only

known difference between AQR and PQR, the descendants of QR and QL, respectively, is that AQR migrates anteriorly and PQR migrates posteriorly. *vab-8* mutations disrupted the posteriorly directed migration of PQR but not the anteriorly directed migration of AQR. Third, *vab-8* mutations disrupted the outgrowth of the posteriorly directed axons of the CAN and PDE neurons, while the anteriorly directed axons of these neurons extended to their normal destinations.

vab-8 mutations had widespread effects on development. The mutations disrupted both cell migrations and axon outgrowth, affected both neuronal and non-neuronal cell types, and disrupted migrations that occur during both embryonic and postembryonic stages of development. The trajectories of these migrations vary in route and environment, occurring in the ventral nerve cord and along the lateral body wall. Thus, the affected cell types have little in common other than migration along the longitudinal axis.

The migration defects in *vab-8* animals are often incomplete and vary in penetrance. For example, although few of the CAN cell bodies reached their normal destination in strong *vab-8* mutants, 17% of CANs in *vab-8(rh205)* animals did migrate a short distance (Fig. 8). Because the strong *vab-8* alleles appear to eliminate all gene activity, we propose that other genes provide or interpret directional information in the absence of *vab-8*. As the elimination of *unc-5*, *unc-6*, or *unc-40* activity also fails to block circumferential migrations completely (Hedgecock et al., 1990), partial redundancy in providing or interpreting directional information might be common to much of *C. elegans* development. Redundancy may also account for the observation that the migrations of RID, M and Z1/Z4 are not affected by *vab-8* mutations.

Although we analyzed the morphology of mature axons, we believe that the premature termination phenotype observed in *vab-8* animals represents a defect in axon outgrowth. We examined the ALA, AVA, AVB, AVD, AVKR and CAN axons, which normally complete outgrowth during embryogenesis, in first and second stage larvae (L1 and L2) and found that these axons extended to relative positions similar to those seen in adults (data not shown). Because adults are much longer than young larvae, these data suggest that these axons do not extend first to their normal positions and then fail to elongate as the animal grows.

Direct and indirect effects of *vab-8* mutations

The observed defects in cell migration and axon outgrowth provide a basis for understanding the behavioral and morphological phenotypes of *vab-8* mutants. The uncoordinated movement phenotype of all *vab-8* mutants is most severe in the posterior body. Because locomotion is controlled by the AVA, AVB, AVD and PVC interneurons (Chalfie et al., 1985), the premature termination of the AVA, AVB and AVD axons in *vab-8* mutants likely contributes to the *vab-8* locomotion defects.

During larval development, the posterior body of strong and weak *vab-8* mutants fails to grow normally, leading to a Wit phenotype. Manser and Wood (1990) proposed that defects in the function of the CAN neurons in the posterior portion of the animal cause the Wit phenotype. *vab-8* strains with more severe CAN migration defects display a more penetrant Wit phenotype, consistent with the hypothesis that the anterior displacement of the CAN cell bodies and axons results in a lack of CAN function in the posterior body that leads to the Wit phenotype.

The reasons for the multivulva and protruding vulva phenotypes of *vab-8* mutants are unclear. A defect in vulval morphogenesis, rather than the generation of the cells that produce the vulva, is likely to cause the Pvl defect (D. Eisenmann, personal communication). *vab-8* might function directly in vulval morphogenesis, or these vulval phenotypes might result indirectly from other *vab-8* defects, such as the withering of the tail. Consistent with the latter possibility, in both strong and weak *vab-8* mutants, all Muv animals are also Wit (B. W., F. Wolf and G. G., unpublished results), and the ectopic ventral protrusions of *vab-8* Muv animals are located posterior to the vulva in the withered body region.

One observation at odds with the model that *vab-8* is required for posteriorly directed migration is that the anteriorly directed PHA and PHB axons typically terminate prematurely in *vab-8* animals. However, similar PHA and PHB axonal defects were observed in *glr-1::mec-4* animals. This observation raises the possibility that in *vab-8* mutants the PHA and PHB outgrowth defects arise as a secondary consequence of the shortening of posteriorly directed axons, such as AVA, AVB and/or AVD. In particular, the AVA and AVD axons are candidates for interacting with PHA and PHB growth cones, because these axons are closely associated, and the AVA and PHB axons synapse extensively (White et al., 1986). However, these experiments do not exclude a direct role of *vab-8* in PHA and PHB outgrowth.

vab-8 functions in a global guidance system along the longitudinal axis

Taken together, our results suggest that *vab-8* encodes or regulates a component of a global signaling system that provides directional information to migrating cells and growth cones. One possibility is that *vab-8* produces or interprets a graded guidance cue distributed along the longitudinal axis. For example, an attractive chemotropic cue might be produced from a source in the tail so that growth cones and migrating cells would migrate posteriorly toward the source (for reviews see Tessier-Lavigne and Placzek, 1991; Tessier-Lavigne, 1994). Alternatively, specific concentrations of a guidance cue might define specific positions along the longitudinal axis. In this model the guidance cue would function similarly to a morphogen for organizing spatial information (Driever and Nüsslein-Volhard, 1988).

Both of these models are similar to those proposed for UNC-6 in *C. elegans* and the netrins in the vertebrate spinal cord, molecules that function in directing growth cones and migrating cells circumferentially. A molecular analysis of the *vab-8* gene should reveal whether *vab-8* encodes a signaling ligand, a receptor, or part of the machinery for producing or responding to the signal. In addition, it will be of interest to determine whether the mechanisms controlling longitudinal guidance are also conserved between nematodes and vertebrates.

We are grateful to Monica Driscoll, Mike Finney, Ed Hedgecock, Ian Hope, Chris Li, James Manser, Barbara Meyer, Gianni Piperno, Fred Wolf, Bill Wood, Jen Zallen, and the *Caenorhabditis* Genetics Center for kindly providing strains and materials used in this work and to David Eisenmann and Fred Wolf for sharing unpublished

results. We also thank Jeff Way and the anonymous reviewers for comments on the manuscript, and members of the Garriga, Meyer and Bargmann laboratories for valuable discussion. This work was supported by a research grant from the Muscular Dystrophy Association, NIH grant NS32057 and a McKnight Scholars Award to G. G. and NIH grant DC01393 to C. I. B. C. I. B. is a Markey Scholar and a Searle Scholar, and some funds for this work were provided by these trusts. C. I. B. is an Assistant Investigator of the HHMI. B. W. was supported by a postdoctoral fellowship from the American Cancer Society, S. G. C. by a postdoctoral fellowship from the Helen Hay Whitney Foundation, W. C. F. by a postdoctoral fellowship from the National Institutes of Health, and A. V. M. by a ADAMHA Scientist Development Award.

REFERENCES

Albertson, D. G. and Thomson, J. N. (1976). The pharynx of *Caenorhabditis elegans*. *Phil. Trans. R. Soc. Lond. B Biol. Sci.* **275**, 299-325.

Brenner, S. (1974). The genetics of *C. elegans*. *Genetics* **77**, 71-94.

Bürglin, T. R. and Ruvkun, G. (1993). The *Caenorhabditis elegans* homeobox gene cluster. *Curr. Opin. Genet. Dev.* **3**, 615-620.

Chalfie, M., Sulston, J. E., White, J. G., Southgate, E., Thomson, J. N. and Brenner, S. (1985). The neural circuit for touch sensitivity in *Caenorhabditis elegans*. *J. Neurosci.* **5**, 956-964.

Chalfie, M., Tu, Y., Euskirchen, G., Ward, W. W. and Prasher, D. C. (1994). Green fluorescent protein as a marker for gene expression. *Science* **263**, 802-805.

Driever, W. and Nüsslein-Volhard, C. (1988). The bicoid protein determines position in the *Drosophila* embryo in a concentration-dependent manner. *Cell* **54**, 95-104.

Driscoll, M. and Chalfie, M. (1991). The *mec-4* gene is a member of a family of genes that can mutate to induce neuronal degeneration. *Nature* **349**, 588-593.

Durbin, R. (1987). *Studies on the Development and Organisation of the Nervous System of Caenorhabditis elegans*, Ph.D. thesis, Cambridge University.

Ferguson, E. L., Sternberg, P. W. and Horvitz, H. R. (1987). A genetic pathway for the specification of the vulval cell lineages of *Caenorhabditis elegans*. *Nature* **326**, 259-267.

Finney, M. and Ruvkun, G. (1990). The *unc-86* product couples cell lineage and cell identity in *C. elegans*. *Cell* **63**, 895-905.

Goodman, C. S. and Shatz, C. J. (1993). Developmental mechanisms that generate precise patterns of neuronal connectivity. *Cell (Suppl.)* **72**, 77-98.

Goodman, C. S. (1994). The likeness of being: phylogenetically conserved molecular mechanisms of growth cone guidance. *Cell* **78**, 353-356.

Greenwald, I. S. and Horvitz, H. R. (1980). unc-93(e1500): A behavioral mutant of *Caenorhabditis elegans* that defines a gene with a wild-type null phenotype. *Genetics* **96**, 147-164.

Hamelin, M., Zhou, Y., Su, M. W., Scott, I. M. and Culotti, J. G. (1993). Expression of the UNC-5 guidance receptor in the touch neurons of *C. elegans* steers their axons dorsally. *Nature* **364**, 327-330.

Hedgecock, E. M., Culotti, J. G., Thomson, J. N. and Perkins, L. A. (1985). Axonal guidance mutants of *Caenorhabditis elegans* identified by filling sensory neurons with fluorescein dyes. *Dev. Biol.* **111**, 158-170.

Hedgecock, E. M., Culotti, J. G., Hall, D. H., and Stern, B. (1987). Genetics of cell and axon migrations in *Caenorhabditis elegans*. *Development* **100**, 365-382.

Hedgecock, E. M., Culotti, J. G. and Hall, D. H. (1990). The *unc-5*, *unc-6* and *unc-40* genes guide circumferential migrations of pioneer axons and mesodermal cells on the epidermis in *C. elegans*. *Neuron* **4**, 61-85.

Ishii, N., Wadsworth, W. G., Stern, B. D., Culotti, J. G. and Hedgecock, E. M. (1992). UNC-6, a laminin-related protein, guides cell and pioneer axon migrations in *C. elegans*. *Neuron* **9**, 873-881.

Kennedy, T. E., Serafini, T., de la Torre, J. R. and Tessier-Lavigne, M. (1994). Netrins are diffusible chemotropic factors for commissural axons in the embryonic spinal cord. *Cell* **78**, 425-435.

Keynes, R. J. and Cook, G. M. W. (1995). Repulsive and inhibitory signals. *Curr. Opin. Neurobiol.* **5**, 75-82.

Kimble, J. and Hirsh, D. (1979). The postembryonic cell lineages of the hermaphrodite and male gonads in *Caenorhabditis elegans*. *Dev. Biol.* **70**, 396-417.

Le Douarin, N. M. (1980). The ontogeny of the neural crest in avian embryo chimeras. *Nature* **286**, 663-669.

Leung-Hagesteijn, H. C., Spence, A. M., Stern, B. D., Zhou, Y., Su, M. W., Hedgecock, E. M. and Culotti, J. G. (1992). UNC-5, a transmembrane protein with immunoglobulin and thrombospondin type 1 domains, guides cell and pioneer axon migrations in *C. elegans*. *Cell* **71**, 289-299.

Loer, C. M. and Kenyon, C. J. (1993). Serotonin-deficient mutants and male mating behavior in the nematode *Caenorhabditis elegans*. *J. Neurosci.* **13**, 5407-5417.

Manser, J. and Wood, W. B. (1990). Mutations affecting embryonic cell migrations in *Caenorhabditis elegans*. *Dev. Genet.* **11**, 49-64.

Maricq, A.V., Peckol, E., Driscoll, M. and Bargmann, C.I. (1995). A candidate glutamate receptor mediates mechanosensory signalling in *C. elegans*. *Nature* **378**, 78-81.

Mello, C., Kramer, J.M., Stinchcomb, D., and Ambros, V. (1991). Efficient gene transfer in *C. elegans*: Extrachromosomal maintenance and integration of transforming sequences. *EMBO J.* **10**, 3959-3970.

McIntire, S. L., Garriga, G., White, J., Jacobson, D. and Horvitz, H. R. (1992). Genes necessary for directed axonal elongation or fasciculation in *C. elegans*. *Neuron* **8**, 307-322.

Nelson, F. K., Albert, P. S. and Riddle, D. L. (1983). Fine structure of the *Caenorhabditis elegans* secretory-excretory system. *J. Ultrastruct. Res.* **82**, 156-171.

Nelson, F. K. and Riddle, D. L. (1984). Functional study of the *Caenorhabditis elegans* secretory-excretory system using laser microsurgery. *J. Exp. Zool.* **231**, 45-56.

O'Rourke, N. A., Dailey, M. E., Smith, S. J. and McConnell, S. K. (1992). Diverse migratory pathways in the developing cerebral cortex. *Science* **258**, 299-302.

Reichardt, L. F. and Tomaselli, K. J. (1991). Extracellular matrix molecules and their receptors: Functions in neural development. *Annu. Rev. Neurosci.* **14**, 531-570.

Schinkmann, K. and Li, C. (1992). Localization of FMRFamide-like peptides in *Caenorhabditis elegans*. *J. Comp. Neurol.* **316**, 251-260.

Serafini, T., Kennedy, T. E., Galko, M. J., Mirzayan, C., Jessell, T. M. and Tessier-Lavigne, M. (1994). The netrins define a family of axon outgrowth-promoting proteins homologous to *C. elegans* UNC-6. *Cell* **78**, 409-424.

Sulston, J. E. and Horvitz, H. R. (1977). Post-embryonic cell lineages of the nematode *Caenorhabditis elegans*. *Dev. Biol.* **56**, 110-156.

Sulston, J. E., Albertson, D. G., and Thomson, J.N. (1980). The *Caenorhabditis elegans* male: Postembryonic development of non-gonadal structures. *Dev. Biol.* **78**, 542-576.

Sulston, J. E., Schierenberg, E., White, J. G. and Thomson, J. N. (1983). The embryonic cell lineage of the nematode *Caenorhabditis elegans*. *Dev. Biol.* **100**, 64-119.

Sulston, J.E. and Hodgkin, J. (1988). Methods. In *The Nematode Caenorhabditis elegans*. (ed. W. B. Wood), Cold Spring Harbor, NY: Cold Spring Harbor Laboratory Press.

Tessier-Lavigne, M., Placzek, M., Lumsden, A. G. S., Dodd, J. and Jessell, T. M. (1988). Chemotropic guidance of developing axons in the mammalian central nervous system. *Nature* **336**, 775-778.

Tessier-Lavigne, M. and Placzek, M. (1991). Target attraction: Are developing axons guided by chemotropism? *Trends Neurosci.* **14**, 303-310.

Tessier-Lavigne, M. (1994). Axon guidance by diffusible repellents and attractants. *Curr. Opin. Gen. Dev.* **4**, 596-601.

Thomas, J. H. (1990). Genetic analysis of defecation in *Caenorhabditis elegans*. *Genetics* **124**, 855-872.

Walsh, C. and Cepko, C. L. (1993). Clonal dispersion in proliferative layers of developing cerebral cortex. *Nature* **362**, 632-635.

Wang, B. B., Muller, I. M., Austin, J., Robinson, N. T., Chisholm, A. and Kenyon, C. (1993). A homeotic gene cluster patterns the anteroposterior body axis of *C. elegans*. *Cell* **74**, 29-42.

White, J. G., Southgate, E., Thomson, J. N. and Brenner, S. (1976). The structure of the ventral nerve cord of *Caenorhabditis elegans*. *Philos. Trans. R. Soc. Lond. B Biol. Sci.* **275**, 327-348.

White, J. G., Southgate, E., Thomson, J. N. and Brenner, S. (1986). The structure of the nervous system of *Caenorhabditis elegans*. *Philos. Trans. R. Soc. Lond. B Biol. Sci.* **314**, 1-340.

Young, J. M. and Hope, I. A. (1993). Molecular markers of differentiation in *Caenorhabditis elegans* obtained by promoter trapping. *Dev. Dyn.* **196**, 124-132.

(Accepted 15 November 1995)